Tuning Cell Adhesion by Incorporation of Charged Silicate Nanoparticles as Cross-Linkers to Polyethylene Oxide[a]

Patrick J. Schexnailder, Akhilesh K. Gaharwar, Rush L. Bartlett II, Brandon L. Seal, Gudrun Schmidt*

Controlling cell adhesion on a biomaterial surface is associated with the long-term efficacy of an implanted material. Here we connect the material properties of nanocomposite films made from PEO physically cross-linked with layered silicate nanoparticles (Laponite) to cellular adhesion. Fibroblast cells do not adhere to pure PEO, but they attach to silicate containing nanocomposites. Under aqueous conditions, the films swell and the degree of swelling depends on the nanocomposite composition and film structure. Higher PEO compositions do not support cell proliferation due to little exposed silicate surfaces. Higher silicate compositions do allow significant cell proliferation and spreading. These bio-nanocomposites have potential for the development of biomedical materials that can control cellular adhesion.

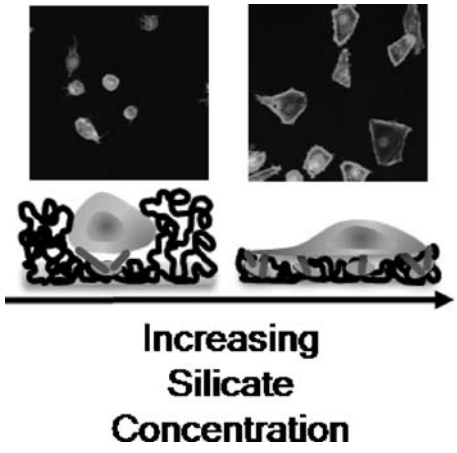

Introduction

Biomedical materials implanted in vivo are subjected to an active environment, where proteins usually coat their surfaces.[1,2] Once a protein coating, through nonspecific binding, is formed, the host immune system will "wall-off" the implant from the rest of the body. This foreign body response can inhibit the efficacy of an implanted biomedical device such as a biosensor or a localized drug depot.[1–3] One approach to reducing this natural immune response is to guide protein and cellular adhesion by surface modification of the implant. Here we show that bio-nanocomposite formulations with defined cellular adhesion properties can be generated by inclusion of charged silicate nanoparticles as cross-linkers to "neutral" poly(ethylene oxide) (PEO) hydrogels. The development of such formulations allows for tailoring consistent cell adhesion properties to a spectrum of potential applications ranging from tissue engineering scaffolds that might desire cell adhesion to drug delivery, biosensor, and cardiovascular stent applications where protein and cell adhesion is unwanted.

Hydrogels made from pure PEOs[4–6] are nonadhesive to mammalian cells, thus these materials can be used to provide blank slates on which to attach macromolecules and incorporate various biomolecules that mediate cellular adhesion.[7] Nonfouling PEOs elicit limited host-immune responses because, in an aqueous environment, a shell of water solvates the polymer molecules which reduces

P. J. Schexnailder, A. K. Gaharwar, R. L. Bartlett II, B. L. Seal, G. Schmidt
Weldon School of Biomedical Engineering, Purdue University, West Lafayette, IN47907, USA
Fax: +1 765 496 1912; E-mail: gudrun@purdue.edu

[a] Supporting information for this article is available at the bottom of the article's abstract page, which can be accessed from the journal's homepage at http://www.mbs-journal.de, or from the author.

DOI: 10.1002/mabi.201000053

protein and cellular interactions with the polymer.[4,7–10] As a result, these polymers, and their derivatives, have been investigated to determine how polymer structure can be controlled to enhance chemical, mechanical, and biological properties.[6,11,12] PEO-based biomaterials have been frequently used as coatings to control cellular adhesion on the surface of other materials,[12,13] but these coatings typically require significant alteration either to the PEO chain itself (e.g., incorporation of adhesion peptide sequences to promote adhesion) or the surface material to which PEO chains are grafted (e.g., PEO brush architectures to reduce adhesion).[11,13–15]

With large-scale production in mind, more recent strategies focus on designing less complicated, more cost-effective biomedical materials that afford controlled cell adhesion.[16] One alternative to the above mentioned fabrication techniques lies in the synergistic combination of nonadhesive synthetic polymers such as PEOs with inorganic, charged nanoparticle cross-linkers that add cellular adhesion sites to the resulting nanocomposite. Further development and property optimization of these materials suggests that there is a clear advantage of this approach over the chemical modification of PEO films with RGD peptide sequences in terms of ease of manufacturing and scalability.

In the past, silicate based glassy materials have been used in the development of biomaterials. For example, a study by Schwarz suggests that silica acts as a cross-linking agent in connective tissue.[17] More recent studies found that the ionic dissolution products of bioactive glass (surface active glass ceramic containing SiO_2, CaO, P_2O_5, etc.) enhance cell proliferation.[18,19] Another study has shown that silicate particles are enzymatically degraded and the degradation products are effectively cleared from the body.[20] Overall, the many findings from literature demonstrate the ability of silicon/silicate to enhance differentiation and proliferation of cells, thus offering new strategies for creating bioactive coatings and scaffolds for tissue engineering.[21,22] We are especially interested in exploring the use of layered silicate nanoparticles (Laponite) in developing bioactive nanocomposite materials. These nanoparticles are synthetic, plate-like silicate poly-ions that reversibly cross-link PEO chains because in aqueous environments the polymer readily adsorbs and desorbs to the nanoparticle surface.[23,24] Additionally, Laponite nanoparticles have been found to degrade into non-toxic products, $Si(OH)_4$, Na^+, Li^+, and Mg^{2+}, under certain pH-dependent conditions,[25,26] which offer opportunities to optimize degradation and dissolution properties as required by specific applications.

The purpose of this paper is to show that cell adhesion properties of PEO based films can be tuned by formulating the composition and structure of bio-nanocomposite hydrogels made from PEO that is cross-linked to charged silicate nanoparticles. In our biomaterials development approach, we combine the chemical properties of silicate (fibroblast cell adhesion) with the favorable characteristics of PEO (nonadhesive to cells) to create hydrogel surfaces that allow for selectively tuned cell adhesion. For the first time with this type of system, we connect the material properties of the samples with the cell adhesive response.

Experimental Part

PEO with a molecular weight ($\overline{M}_w$) of 10^6 g·mol^{-1} and a polydispersity index of 1.5 was purchased from Polysciences, Inc. Laponite RD (LRD) from Southern Clay Products, Inc., is a synthetic Hectorite-type silicate consisting of nano platelets with an average diameter of 25–30 nm and a thickness of approximately 1 nm. Laponite cross-linked PEO films were prepared via gel/solution exfoliation while optimal solutions were obtained for a particular polymer silicate ratio, pH, and ionic strength.[27] For this work we initially prepared hydrogels composed of X wt.-% PEO, $5 - X$ wt.-% LRD and 95 wt.-% water at ambient temperature. The solution pH and ionic strength in the hydrogel were controlled by adding 10^{-4} M NaOH and 10^{-3} M NaCl, respectively. Hydrogels were manually spread onto glass slides and dried at 25 °C in desiccators and subsequently under vacuum.[27] The composition of films after solvent evaporation was calculated from the initial weight of polymer and silicate (by mass fraction), listed in Table 1. After drying, all films were 70–100 μm thick. Polarized microscopy was done using an Olympus BX51 microscope (Olympus, Melville, NY, USA) with the application of a first order wavelength gypsum plate.

The hydration behavior of nanocomposite films was assessed in phosphate-buffered saline (PBS) at ambient temperature (≈23 °C) and at 37 °C for 24 h. The mass change during the course of swelling was monitored by measuring the mass of the swollen nanocomposite. The hydration degree was characterized using the following equation:

$$\text{Hydration degree} = \frac{(M_{wet} - M_{init}) \times 100}{M_{init}}$$

where M_{init} is the initial weight and M_{wet} is the wet weight of the nanocomposite films.

Table 1. Formulations and diffusion characteristics of polymer nanocomposites, where *k* is the characteristic swelling constant and *n* is the characteristic exponent describing the mode of solvent transport. Samples are named X% Silicate.

[Silicate]	[PEO]	[LRD]	*n*	*k*
%	%	%		
20	80	20	0.28	0.26
30	70	30	0.28	0.26
40	60	40	0.24	0.30
50	50	50	0.16	0.47
60	40	60	0.10	0.60
70	30	70	0.09	0.61

Macromolecular Journals
DOI: 10.1002/mabi.201000053

NIH 3T3 mouse fibroblast cells were purchased from American Type Culture Collection (ATCC). Cells were grown in Dulbecco's modified eagle medium (DMEM) supplemented with 10% bovine calf serum, 100 $U \cdot mL^{-1}$ penicillin, 100 $\mu g \cdot mL^{-1}$ streptomycin, and 4×10^{-3} M L-glutamine (Sigma). Serum free experiments were cultured in DMEM supplemented with 4×10^{-3} M L-glutamine. Films were cut into 1.5 cm circular discs, briefly submersed in 70% ethyl alcohol and then allowed to dry under sterile conditions for all experiments. Before seeding, films were placed in multiwell plates and immersed in cell culture media overnight. For growth curve experiments, films were seeded at 7 500 cells $\cdot cm^{-2}$ in ultra-low attachment 24-well plates (Corning). Cell number was estimated by incubation with CellTiter 96 aqueous one solution cell proliferation assay (Promega) following the manufacturer's protocol. For viability experiments, films were seeded at 7 500 cells $\cdot cm^{-2}$ in black-walled, 24-well plates (Greiner Bio-One). Cell viability was determined using the MultiTox-Fluor multiplex cytotoxicity assay (Promega) following the manufacturer's protocol. For adhesion experiments, cells were seeded at 20 000 cells $\cdot cm^{-2}$. After 3 h, cells were fixed using 3.7% formaldehyde solution. The cellular cytoskeleton was labeled with Alexa Fluor 488 phalloidin, and the nucleus was counterstained with 7-aminoactinomycin D (Invitrogen). Fluorescent images were taken with an Olympus FV1000 confocal microscope. Representative images are shown. To evaluate cell spreading as a function of nanocomposite composition, raw confocal images were converted into black and white images using a threshold. Then the cumulative area fraction was obtained from the processed image using ImageJ software (NIH).

Hemocompatibility analysis of nanocomposite films was conducted in pooled bovine whole blood containing Na^+ citrate (Innovative Research, Inc.) that was used within 24 h. Coagulation was measured with a HEMOCHRON® Response whole-blood coagulation system to calculate the activated partial thromboplastin time. Sample nanocomposite films were pulverized with a mortar and pestle and then dissolved in Milli-Q water for testing. HEMOCHRON® tubes containing colloidal kaolin activating agent and 0.02% Thimerosal preservative agent were dosed with 2 mL blood and 200 μL sample with a concentration of 10 $mg \cdot mL^{-1}$ sample. Coagulation controls were measured by adding 200 μL Milli-Q water or 200 μL of 0.01 $mg \cdot mL^{-1}$ heparin.

Statistical analysis was performed using SAS version 9.1.3 (SAS Institute, Cary, NC) to determine statistical difference. A two sample *t*-test was performed using the Satterthwaite approximation due to unequal variances. P values < 0.05 were deemed significantly different.

Results and Discussion

The chemical composition and structural morphology of the nanocomposite films studied here are important parameters that influence the cell adhesion properties. Polarized optical microscopy images in Figure 1a show birefringent spherulites that indicate the presence of polymer crystals within the dried nanocomposite films

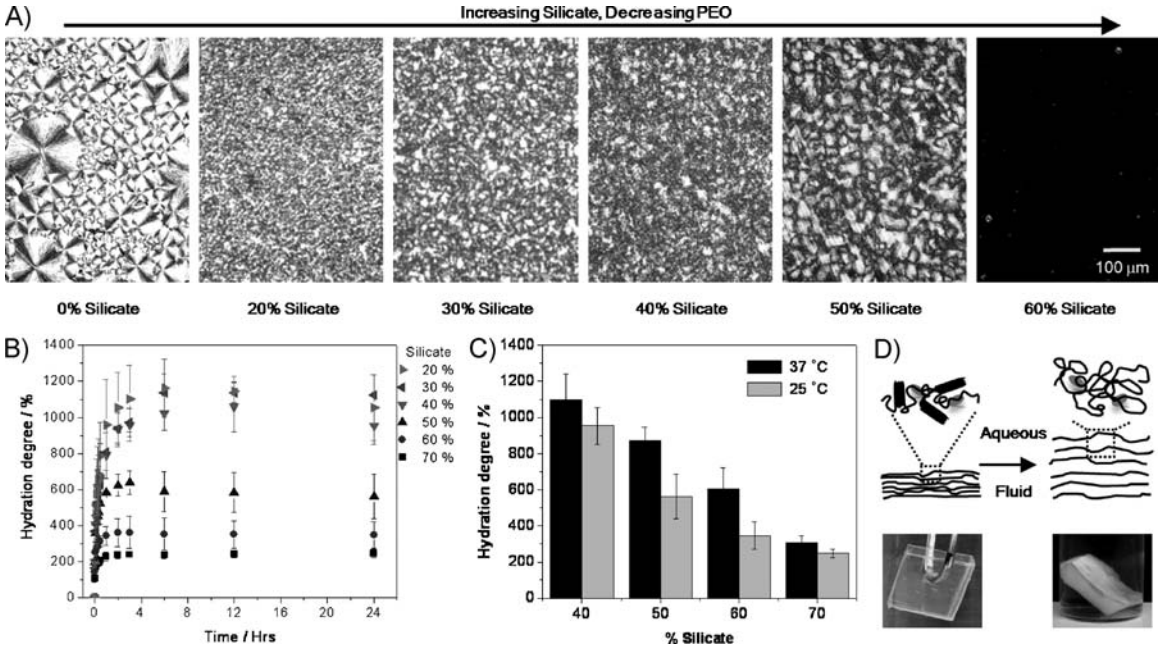

Figure 1. Composition alters the structural and swelling properties of bio-nanocomposite films which is critically important to the cell adhesion properties. (A) Due to the crystalline nature of PEO, pure PEO films exhibit highly birefringent spherulites of considerable size. With addition of silicate, spherulite size decreases indicating a reduction in PEO crystallinity. With a further decrease in polymer loading (40% PEO, 60% silicate), no birefringent crystalline phase was observed. Scale bar is consistent throughout. (B) Nanocomposite films swell to greater degrees with decreasing silicate composition at 23 °C. The equilibrium hydration ratio decreases from 1150% for 20% silicate to 220% for 70% silicate. The decrease is attributed to increased cross-linking density and to decreased polymer capable of swelling. (C) Similar hydration trend was observed at both 23, 25, and 37 °C after 24 h, although the hydration kinetics were faster at physiological temperature. (D) Immersion of dried films in an aqueous fluid causes the PEO crystallites to become amorphous and swell. A multilayered film structure forms.[34]

before immersion in PBS. Under dry conditions, neat PEO films are highly crystalline, making these films opaque as the PEO spherulite sizes are much larger than the length scale of the scattered visible light. Birefringence, as seen in Figure 1, usually originates from the orientation of anisotropic structures such as elongated polymer chains, from oriented or crystallized polymer domains, or from aligned nanoparticles.[28] In pure PEO, spherulites are observed due to the radial growth of polymer lamellae from crystal nucleation sites. Addition of a small amount of silicate nanoparticles (20%) significantly decreases the amount and size of spherulites, a behavior which has been observed by other research groups.[29,30] The birefringent areas representing PEO crystallites (Figure 1) allows us to estimate the size and number of PEO rich areas after the dried nanocomposite film is immersed in PBS and polymer crystallinity is lost. These birefringent and PEO rich areas, should support cell adhesion less compared to the non-birefrigent, silicate-nanoplatelet-rich areas.

A further increase in silicate concentration (up to 50%) reduces the total birefringence, but increases the spherulite size (Figure 1a). According to published work, this effect may be attributed to amorphous PEO chains adsorbed to the surface of the silicate, which slow down the overall crystallization kinetics by decreasing the number of nucleation sites within the polymer matrix and lead to larger, but fewer, polymer crystals.[29,31] At a silicate concentration of 60% or higher, birefringence drops drastically suggesting that the PEO within the nanocomposite films is amorphous and that any remaining crystallites that might be sandwiched between silicate nanoplatelets cannot be detected by polarized microscopy (no birefringence visible). Previous studies have shown that a ratio of 60% silicate to 40% PEO is sufficient to fully cover all silicate nanoparticle surfaces within a hydrogel[23,24,32,33] as well as within a film made from dried hydrogel.[34] For example, freeze fracture TEM images, from the network like hydrogel show that the mesh size of the network is ca. 50–80 nm, in agreement with previously obtained small angle neutron scattering.[32,33] The thickness of visualized strings is ca. 4 nm while the thickness of single Laponite platelets is ca. 1 nm. Interpreting these lines as polymer coated platelets viewed from the side leads to an adsorbed layer thickness of 1.5 nm on each side.[32,33] Although PEO interacts with the silicate nanoparticles, we show in the following, that fibroblast cells preferentially attach to nanocomposite films that have silicate concentrations of 50% or higher.

After nanocomposite films are immersed in PBS, polymer crystallinity is lost and swelling leads to the formation of hydrogel films. The hydration and swelling of these films are important for cell adhesion and growth as the hydration degree directly influences the material surface properties. The hydration behaviors of the film compositions used for cell growth experiments are summarized in Figure 1b–d. Hydration behavior was assessed at 23 °C, which is important to the processing and storage conditions, and at 37 °C to represent body temperature. Since both PEO and Laponite are hygroscopic, all nanocomposite films hydrate quickly in a PBS solution, and reach equilibrium within 6 h (Figure 1b and d). The hydration degree is defined as the weight ratio of the net liquid uptake to the dried nanocomposite film. The equilibrium hydration degree of the films decreases with increasing silicate concentration and increases at physiological temperature (Figure 1c). This trend, as a function of silicate composition, is mainly attributed to the formation of a denser cross-linked network between the PEO polymer chains and silicate cross-linkers. Our previous mechanical testing and small angle neutron scattering studies have shown that experimental results are highly reproducible within a time frame of at least three months[35] and that degradation/dissolution effects of the PEO silicate network can be neglected during the timeframe of the sample preparation and experiments presented here.[35] The molecular weight of the model PEO chosen is too high to degrade within the experimental timeframe and the very slow dissolution of the cross-linking silicate nanoparticles does not affect the cell adhesion studies shown here. A pure PEO film control, not shown here, quickly dissolves in PBS. The transport properties of solvent within the nanocomposite networks were determined by fitting the initial hydration data to the expression

$$\frac{M_t}{M_{eq}} = kt^n$$

where M_t is the mass of water uptake at time t, M_{eq} the equilibrium water uptake, k the characteristic swelling constant and n is the characteristic exponent describing mode of water transport.[36] A value of $n \leq 0.5$ indicates Fickian diffusion, $0.5 < n < 1$ indicates non-Fickian diffusion (where diffusion and polymer relaxation both control the overall water uptake) and $n = 1$ indicates relaxation controlled transport. The values of n and k for different nanocomposite compositions are listed in Table 1. The fitting data suggest Fickian diffusion for all nanocomposite hydrogels measured, indicating that therapeutic agents can potentially be delivered with this system after further material development. However, the adsorption of macromolecular drugs[37] or proteins to the charged silicate platelets as well as compositional changes may further influence the release kinetics, although this will be mainly a composition dependent process.[38]

Figure 2 summarizes results obtained from cells grown on the surface of the swollen nanocomposite films previously discussed. These results show that the adhesion and cell growth of NIH 3T3 fibroblasts can be controlled by simply changing the ratio of PEO to silicate of a hydrogel

Macromol. Biosci. 2010, 10, 000–000

Macromolecular Journals
DOI: 10.1002/mabi.201000053

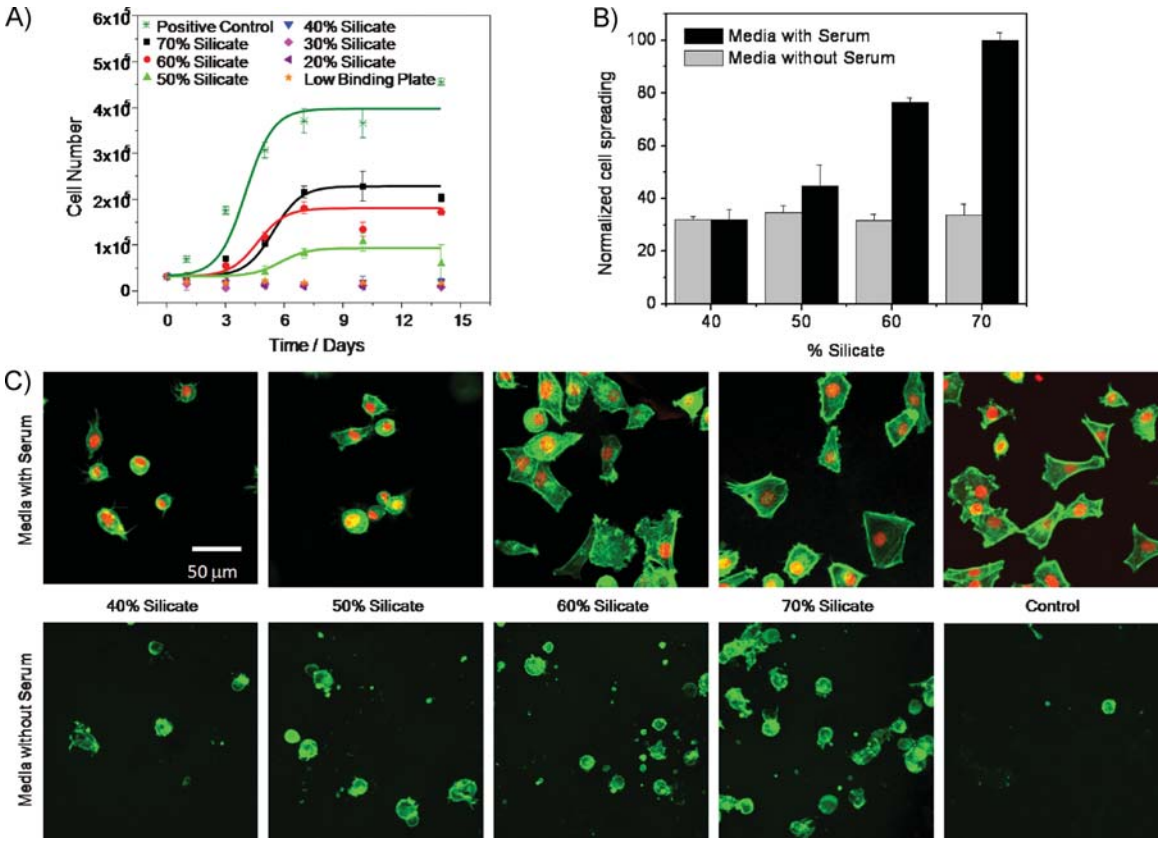

Figure 2. Cell proliferation and spreading depend on silicate concentration. (A) Fibroblast cells proliferate to a greater extent on films containing higher silicate concentrations. Decreasing PEO concentration results in increased cell number with time. Sigmoidal fitting for 50–70% silicate provided as a guide to the eye. There is not a significant number of cells growing on the surface of films containing $\leq$40% silicate. For 50–70% silicate samples, the number of cells in the plateau phase of the growth curve is proportional to the silicate concentration. (B) Cells spread more (quantified by the area cells encompass and normalized by both spreading area and cell number to the 70% silicate group) as the silicate composition of films increases when cultured in serum containing media. All serum containing groups are significantly different from each other ($n = 4$, $p < 0.05$), except 40–50% silicate. When cultured in serum free media, normalized cell spreading is not significantly different. (C) Representative confocal images showing an increase in cell number and cell spreading with increasing silicate concentration after 3 h of incubation with serum containing media (top) and with serum free media (bottom). Cells seeded at 20 000 cells $\cdot$ cm^{-2}.

film. Cells readily adhere, grow and proliferate on the film surfaces that contain more than 40 wt.-% of silicate (Figure 2a) while hydrogel films containing 40 wt.-% silicate, or less, show little cell adhesion and growth. The viability of cells on all hydrogel surfaces remained high, at $\approx$95%, throughout the 14-d experimental period when seeded in normal tissue culture plates (Table 2), indicating the change in composition is not cytotoxic to cells. Because nonfouling PEO surfaces resist protein adsorption as well as mammalian cell adhesion,[9,10] the presence of layered silicate nanoparticles must be responsible for the increased adhesion of cells.[22] For the samples having higher silicate compositions, normal cell spreading was observed with indications of focal adhesions. Overall, increased cell spreading was observed with increased concentration of nanoparticles (Figure 2b and c, top), and the cell spreading was found to be statistically different between all groups

Table 2. Cell viability of fibroblast cells remains unchanged when seeded on different compositions of multilayered films. Initial seeding viability 96.4 $\pm$ 0.8% (average viability $\pm$ standard deviation, $n = 3$).

Sample	Cell viability		
	%		
	Day 1	Day 7	Day 14
40% silicate	95.5 $\pm$ 0.2	96.1 $\pm$ 0.1	98.0 $\pm$ 0.6
50% silicate	91 $\pm$ 1	96.5 $\pm$ 0.7	97.7 $\pm$ 0.5
60% silicate	91 $\pm$ 3	97 $\pm$ 1	97.3 $\pm$ 0.3
70% silicate	85 $\pm$ 2	95.9 $\pm$ 0.7	97.2 $\pm$ 0.3
TCPS	92 $\pm$ 3	94.1 $\pm$ 0.7	94.3 $\pm$ 0.9

($p < 0.05$), except the 40 and 50% silicate, when grown in the presence of serum.

In order to determine the role of serum proteins play in fibroblast adhesion to these polymer nanocomposites, such as vitronectin which readily binds to glass and mediate cell adhesion through integrin binding domains,[39] selected cell adhesion studies were performed under serum free conditions. It is well known that functional cell adhesion to materials is mediated through cell-membrane receptors, typically from the integrin family. The integrin recognition of adhesion sites (RGD sequences) are very specific, e.g., distinguishing between native peptide sequences and their scrambled analogues.[12,14] Experimental results show that some fibroblast attachment takes place even under serum free conditions and follows a silicate concentration dependent trend, although cells seeded under these conditions do not exhibit proper adhesion morphology, with a spherical shape and no signs of functional adhesion (Figure 2c, bottom, Figure S1 and S2 in Supporting Information). Very few adherent cells were observed on tissue culture polystyrene (TCPS), and cells could not be seeded to the "uncross-linked" PEO polymer alone, as a pure PEO film control quickly dissolves. A covalently cross-linked PEO diacrylate control does not show cell adhesion. The difference in cell morphology, under different serum conditions, clearly shows the decisive role adsorbed proteins play in mediating the difference between materials with increasing content of silicate particles. This suggests that cell adhesion is supported by cell adhesion sites created by adhesion of proteins to the silicate surfaces. In order to further our understanding on this issue, future studies will investigate the specific cell/matrix interactions involved with cellular adhesion in this system.

In Figure 2a it was shown that for the samples containing 50–70% silicate, the number of cells in the plateau phase of the cell growth curve is proportional to the silicate concentration. Given that the samples containing more silicate led to more spread cell morphology one could expect that these samples should also lead to lower number of cells in the plateau region. However our observations suggest that this is not the case and that cells grown on the nanocomposite surface do not reach confluency when the plateau phase is reached (Figure 3). The plateau is not a result of contact inhibition of a confluent cell layer (after 6 d), and we attribute the growth inhibition is dictated by the amount and distribution of "cell repellant" PEO and "cell adhesive silicate" areas on the hydrogel surface (Figure 1a). This can be explained by differences in "protein repellant" PEO and "protein adhesive silicate" regions, as serum protein mediates fibroblast cell adhesion. Protein adsorption experiments show proteins do adsorb to the nanocomposite samples (data not shown). However, the results of these experiments are clouded by the large difference in sample swelling (Figure 1b), making an accurate quantification of adsorbed protein, as a function of silicate composition, difficult. Regardless, the silicate concentration dependent decrease in cell number observed in the plateau phase of the growth curve seems to be dominated by the availability of silicate rich surfaces for cell adhesion and growth, and less due to differences in cell spreading. This conclusion is based upon the number of cells observed in the plateau phase of the growth curve seeded upon nanocomposite samples and tissue culture polystyrene control groups (Figure 2a). The lack of higher cell numbers in the plateau phase of experimental groups, as well as the significantly higher number of cells and the degree of cell spreading in the positive control group, indicates the area available for cell growth decreases with increasing polymer composition.

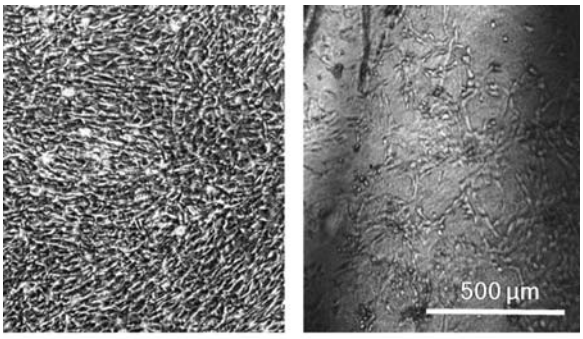

Figure 3. Cell distribution 6 d post-seeding changes depending on substrate. As cell number approaches plateau phase of growth curve (Figure 2), cells are contact-inhibited in TCPS (tissue culture polystyrene). In nanocomposite samples, cells are not confluent. Rather, the surface area available for cellular attachment (silicate-rich regions) decreases with increasing polymer concentration. Cells seeded at 25 000 cells · cm^{-2}.

Additionally, actin stress fibers can be seen on cells grown on high silicate samples (60 and 70% silicate), but these structures are not present on lower silicate samples (Figure 2c and 4a). The presence of stress fibers under tissue culture polystyrene control and high silicate conditions indicates the presence of mature cell-matrix adhesion complexes on the surface of films containing a high concentration of silicate.[40] Overall, these results indicate that fibroblast cells need high silicate concentrations to proliferate and adopt a typical in vitro morphology. Lower silicate concentrations yield a reduction in cell adhesion and spreading, but the overall cell viability remains constant across all groups (Table 2).

Previous work on similar LRD-PEO hydrogel systems showed that PEO molecules dynamically adsorb and desorb off the surfaces of layered silicate nanoparticles while at the same time competing for the silicate surfaces with non adsorbed polymer chains.[32,33] Assuming this adsorption-desorption equilibrium also applies to the swollen nanocomposite hydrogel films studied here, one would expect

Macromol. Biosci. **2010**, *10*, 000–000

DOI: 10.1002/mabi.201000053

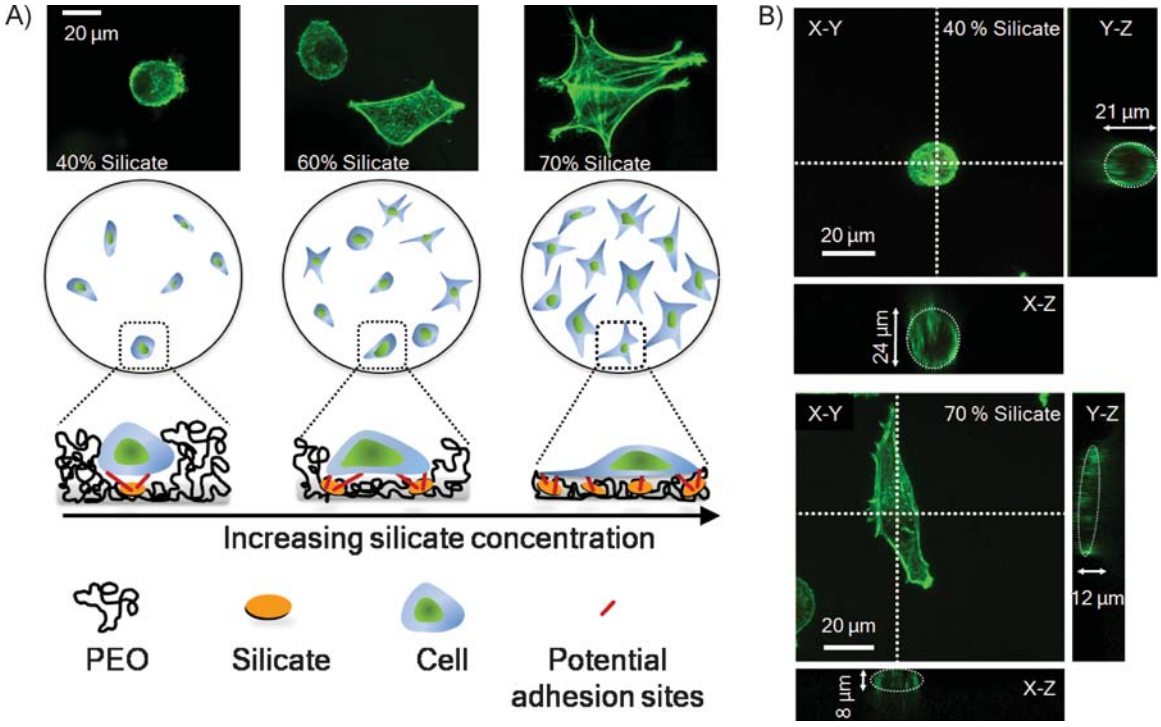

Figure 4. Cell adhesion and spreading depend on silicate concentration. (A) Upon immersion in culture media, the polymer chains undergo a dynamic adsorption-desorption mechanism with the silicate surface. Bio-nanocomposite films with low silicate concentrations (left) swell to a high degree. Swollen PEO chains discourage cell/silicate interaction, reducing cell adhesion and spreading. With increasing silicate concentration, films do not swell to the same degree, and increased numbers of silicate nanoparticles provide potential cell adhesion sites. (B) Representative *X-Z* and *Y-Z* cross sections, highlighted by dotted lines, of 40% silicate (top) and 70% silicate (bottom) indicate that cells flatten to a greater degree with higher silicate compositions, supporting the proposed cell-material interaction scheme.

that with an increase in PEO concentration, fewer silicate regions are available as potential protein and cell adhesion sites (Figure 4a). As the PEO composition is increased, fewer silicate nanoparticles have regions that are in an "unbound" state, resulting in a smaller probability for cells to have successful interactions with silicate surfaces. This effect is reflected in the decrease in cell numbers during the plateau phase of the growth curve as well as the decrease in cell spreading (Figure 2). Additionally, excess PEO (crystalline) regions lead to PEO rich areas on the film surface, which are nonadhesive to cells. Further support of the cell adhesion properties of the nanocomposite can be seen in Figure 4b, which shows the three dimensional spreading of cells seeded on representative 40 and 70% silicate samples. In addition to spreading to a higher degree, cells seeded on the 70% silicate sample flatten to the substrate surface due to mature cell-substrate binding, whereas the spherical morphology of cells seeded on high PEO compositions are indicative of poorer cell/nanocomposite interaction.

Finally, activated clotting time experiments were performed to determine if the silicate nanoparticles interact with the intrinsic coagulation cascade. Usually silicates will be effective activators of the intrinsic coagulation cascade, which is important even in non-blood contact applications. While natural silicate materials such as Kaolin are known to initiate the coagulation cascade, our experiments suggest that the polymer/silicate nanocomposite does not lead to a decrease in activated clotting time (Table 3). Kaolin silicates are thought to initiate the clotting cascade due to anionic silicate surfaces activating factor XII (Hageman factor).[41] In the system presented here, Laponite nanoparticles may not initiate the coagulation

Table 3. Activated clotting time of nanocomposite samples at 10 mg · mL^{-1} concentration. Heparin added at 0.01 mg · mL^{-1} (average viability ± standard deviation, $n = 3$).

Sample	Activated clotting time
	s
70% silicate	223 ± 15
60% silicate	211 ± 6
50% silicate	205 ± 11
40% silicate	225 ± 10
water	221 ± 9
heparin	>1 000

cascade because Laponite has additional cationic charges compared to Kaolin and PEO chains interacting with the surface of the silicate particles prevent the activation of factor XII.

Conclusion

We conclude that cell adhesion properties can be tuned by formulating the composition and structure of bionanocomposite hydrogel films made from PEO that is crosslinked to charged silicate nanoparticles (Laponite). On the macroscale, the polymer crystallinity of the films observed in the dried state allows for determining PEO rich areas in the swollen film state; these areas are less adhesive to cells than the silicate rich nanocomposite hydrogel surfaces. At smaller length scales, the adsorption properties of PEO polymer chains to the silicate surfaces also influence the adhesion of cells. Thus our feasibility study suggests that the ability to regulate cellular attachment to the bionanocomposite film surfaces can be tailored toward the specific requirements of a biomedical application.

Acknowledgements: The authors thank Prof. *O. Akkus* of the *Weldon School of Biomedical Engineering, Purdue University,* for use of his polarized microscope and Ms. *Christine Gustafson* for sample preparation. Work by the authors was supported by an *NSF-CAREER* award 0711783, to GS and by a Purdue Lynn Doctoral fellowship to PS. The authors declare that they have no conflict of interest.

Received: February 3, 2010; Revised: March 29, 2010; Published online: DOI: 10.1002/mabi.201000053

Keywords: adhesion; biocompatibility; layered silicates; nanocomposites; nanoparticles

[1] D. G. Castner, B. D. Ratner, *Surf. Sci.* **2002**, *500*, 28.
[2] C. J. Wilson, R. E. Clegg, D. I. Leavesley, M. J. Pearcy, *Tissue Eng.* **2005**, *11*, 1.
[3] K. S. Jones, *Semin. Immunol.* **2008**, *20*, 130.
[4] J. M. Harris, "*Poly(ethylene glycol) Chemistry: Biotechnical and Biomedical Applications*", Plenum Press, New York, London 1992.
[5] P. J. Schexnailder, G. Schmidt, *Colloid Polym. Sci.* **2009**, *287*, 1.
[6] B. L. Seal, T. C. Otero, A. Panitch, *Mater. Sci. Eng. R* **2001**, *34*, 147.
[7] B. V. Slaughter, S. S. Khurshid, O. Z. Fisher, A. Khademhosseini, N. A. Peppas, *Adv. Mater.* **2009**, *21*, 3307.
[8] M. C. Cushing, K. S. Anseth, *Science* **2007**, *316*, 1133.
[9] G. M. Harbers, K. Emoto, C. Greef, S. W. Metzger, H. N. Woodward, J. J. Mascali, D. W. Grainger, M. J. Lochhead, *Chem. Mater.* **2007**, *19*, 4405.
[10] E. Tziampazis, J. Kohn, P. V. Moghe, *Biomaterials* **2000**, *21*, 511.
[11] J. K. Tessmar, A. M. Göpferich, *Macromol. Biosci.* **2007**, *7*, 23.
[12] J. K. Tessmar, A. M. Göpferich, *Adv. Drug Delivery Rev.* **2007**, *59*, 274.
[13] C. D. Heyes, J. Groll, M. Möller, G. U. Nienhaus, *Mol. Biosyst.* **2007**, *3*, 419.
[14] H. Shin, S. Jo, A. G. Mikos, *Biomaterials* **2003**, *24*, 4353.
[15] M. Zhang, T. Desai, M. Ferrari, *Biomaterials* **1998**, *19*, 953.
[16] E. S. Place, D. E. Nicholas, M. M. Stevens, *Nat. Mater.* **2009**, *8*, 457.
[17] K. Schwarz, *Proc. Natl. Acad. Sci. USA* **1973**, *70*, 1608.
[18] T. J. Gao, H. T. Aro, H. Ylanen, E. Vuorio, *Biomaterials* **2001**, *22*, 1475.
[19] I. D. Xynos, A. J. Edgar, L. D. K. Buttery, L. L. Hench, J. M. Polak, *J. Biomed. Mater. Res.* **2001**, *55*, 151.
[20] W. Lai, J. Garino, P. Ducheyne, *Biomaterials* **2002**, *23*, 213.
[21] W. Helen, C. L. R. Merry, J. J. Blaker, J. E. Gough, *Biomaterials* **2007**, *28*, 2010.
[22] H. M. Lewkowitz-Shpuntoff, M. C. Wen, A. Singh, N. Brenner, R. Gambino, N. Pernodet, R. Isseroff, M. Rafailovich, J. Sokolov, *Biomaterials* **2009**, *30*, 8.
[23] A. Nelson, T. Cosgrove, *Langmuir* **2004**, *20*, 10382.
[24] A. Nelson, T. Cosgrove, *Langmuir* **2004**, *20*, 2298.
[25] V. Castelletto, I. A. Ansari, I. W. Hamley, *Macromolecules* **2003**, *36*, 1694.
[26] D. W. Thompson, J. T. Butterworth, *J. Colloid Interface Sci.* **1992**, *151*, 236.
[27] E. A. Stefanescu, P. J. Schexnailder, A. Dundigalla, I. I. Negulescu, G. Schmidt, *Polymer* **2006**, *47*, 7339.
[28] A. K. Gaharwar, P. Schexnailder, V. Kaul, O. Akkus, D. Zakharov, S. Seifert, G. Schmidt, *Adv. Funct. Mater.* **2009**, *20*, 429.
[29] W. Loyens, P. Jannasch, F. H. J. Maurer, *Polymer* **2005**, *46*, 915.
[30] D. Ratna, S. Divekar, A. B. Samui, B. C. Chakraborty, A. K. Banthia, *Polymer* **2006**, *47*, 4068.
[31] K. E. Strawhecker, E. Manias, *Chem. Mater.* **2003**, *15*, 844.
[32] E. Loizou, P. Butler, L. Porcar, E. Kesselman, Y. Talmon, A. Dundigalla, G. Schmidt, *Macromolecules* **2005**, *38*, 2047.
[33] E. Loizou, P. Butler, L. Porcar, G. Schmidt, *Macromolecules* **2006**, *39*, 1614.
[34] A. Dundigalla, S. Lin-Gibson, V. Ferreiro, M. M. Malwitz, G. Schmidt, *Macromol. Rapid Commun.* **2005**, *26*, 143.
[35] E. Loizou, L. Porcar, P. Schexnailder, G. Schmidt, P. Butler, *Macromolecules* **2010**, *43*, 1041.
[36] P. L. Ritger, N. A. Peppas, *J. Controlled Release* **1987**, *5*, 23.
[37] C. J. Wu, G. Schmidt, *Macromol. Rapid Commun.* **2009**, *30*, 1492.
[38] W. F. Lee, Y. T. Fu, *J. Appl. Polym. Sci.* **2003**, *89*, 3652.
[39] E. G. Hayman, M. D. Pierschbacher, Y. Ohgren, E. Ruoslahti, *Proc. Natl. Acad. Sci. USA* **1983**, *80*, 4003.
[40] K. Burridge, M. Chrzanowska-Wodnicka, *Annu. Rev. Cell Dev. Biol.* **1996**, *12*, 463.
[41] E. A. Vogler, C. A. Siedlecki, *Biomaterials* **2009**, *30*, 1857.